Effect of pH buffer molecules on the light-induced currents from oriented purple membrane

S. Y. Liu, M. Kono, and T. G. Ebrey
Department of Physiology and Biophysics, University of Illinois, Urbana, Illinois 61801 USA

ABSTRACT The effect of pH buffers on the microsecond photocurrent component, B2, of oriented purple membranes has been studied. We found that under low salt conditions (<10 mM monovalent cationic salt) pH buffers can dramatically alter the waveform of the B2 component. The effect is induced by the protonation process of the buffer molecules by protons expelled from the membrane. These effects can be classified according to the charge transition upon protonation of the buffer. Buffers that carry two positive charges in their protonated form add a negative current component (N component) to B2. Almost all of the other buffers add a positive current component (P component) to B2, which is essentially a mirror image of the N component. Buffers with a pK <5.5 have only a small positive buffer component. The pH dependence of the buffer effect is closely related to the pK of the buffer; it requires that the buffer be in its unprotonated form. The rise time of the buffer component increases with the concentration of the buffer molecules. All the buffer effects can be inhibited by the addition of 5 mM of a divalent cation such as Ca^{2+}. Reducing the surface potential slows down the N component but accelerates the P component without affecting the amplitude of the buffer effect significantly. Many of the buffer effects can be explained if we assume that upon protonation of the buffer by a proton expelled from the membrane by light, the buffer molecules move toward the membrane. This backward movement of buffer molecules forms a counter current very similar to that due to cations discussed in Liu, S. Y., R. Govindjee, and T. G. Ebrey. (1990. *Biophys. J.* 57:951–963).

INTRODUCTION

Bacteriorhodopsin, a light-driven proton pump, is one of the most extensively studied membrane proteins. The purple membrane (PM) in which it resides has a large negative surface charge density at neutral pH due to the negatively charged amino acid residues and lipid molecules on its surface. Upon illumination, bacteriorhodopsin undergoes a cycle of discrete intermediate states which can be monitored spectroscopically. During this photocycle a proton is released into the external media, and one is taken up from the cytoplasmic side. The net vectorial movement of protons is a major contributor to an electrical signal which contains three main components. Recent work from this laboratory has characterized the microsecond component (B2) of this signal, which correlates well with the L-M optical photocycle transition under high salt conditions; we concluded that it arises directly from proton movement (Liu, 1990; Liu et al., 1990; see also Keszthelyi and Ormos, 1989; for a review see Trissl, 1990). However, when the salt concentration is low the B2 component is altered even though the optical signal is not. This finding has led to a "counter-current" model (Liu et al., 1990; see also Marinetti, 1987) in which a transient increase in the negative surface charge after proton release leads to the attraction of a cation back towards the surface in opposition to the proton current, a phenomenon that can be readily detected at low ionic strengths by photocurrent measurements (Liu et al., 1990).

In addition to low salt concentrations, pH buffers also alter the electrical signal (Liu et al., 1990). The interaction between released protons from the PM and a buffer in the bathing solution has not been carefully studied, although some unusual relationships have been noticed by several investigators. Drachev et al. (1984), for example, found faster kinetics of the light-induced proton release signal detected by a pH indicator in the presence of a pH buffer. Marinetti and Mauzerall (1983) reported that during the photocycle of bacteriorhodopsin there is a conductivity signal that cannot be suppressed by a pH buffer at pH 8; they proposed that there is a large nonproton ion release during the photocycle. Tóth-Boconádi et al. (1986) and Dér et al. (1988) reported that in the presence of diamines, a category of pH buffers that become divalent cations when protonated, the microsecond and millisecond range photocurrent signals change sign. They proposed that the proton pump is reversed by diamines, although alternative explanations have been suggested (Marinetti, 1987; Liu et al., 1990). Because the photocycle of bacteriorhodopsin involves proton transport across the membrane, the correct interpretation of the results of photo-

0006-3495/91/07/204/13 $2.00

current measurements in the presence of pH buffers is difficult but may give us quite useful information.

In this paper, the effects of 31 different kinds of pH buffers on the microsecond component (B2) of bacteriorhodopsin's photocurrent were studied. With high salt concentrations, the B2 component is primarily due to light-initiated proton release from the PM into the external bathing solution. At lower salt concentrations, we find that this waveform is altered in the presence of almost all of the buffers and call this change the buffer effect. The type and degree of this effect is dependent on the buffer used, salt concentration, pH, the buffer's pK, and surface charge of the PM.

Our results suggest that the buffer effect represents the charge movement and/or the dipole change of buffer molecules close to the surface of the protein. A counter current model, in which negative charges left near the surface of PM after proton release cause movement and reorientation of the buffer molecules, can explain most of the phenomena observed.

MATERIALS AND METHODS

PM was prepared from *Halobacterium halobium* strain S-9 cells according to the method of Becher and Cassim (1975), omitting the DNase treatment.

Immobilization of PM in a polyacrylamide gel was done essentially by the method of Dér et al. (1985) except that the final concentration of ammonium persulfate was 0.25% (Liu and Ebrey, 1988). Orientation and conditions of the PM during polymerization are described by Liu (1990). Briefly, the acrylamide solution containing 30 μM bacteriorhodopsin was polymerized as a single large 60 × 4.9 × 50 mm piece with a 15 V/cm orientation voltage. This gel was washed in distilled water for at least 48 h before it was cut into the 6 × 4.9 × 12 mm pieces used for measurements. Pieces with air bubbles or obvious inhomogeneities were discarded.

The experimental setup for the photocurrent and optical measurements was identical to that described previously (Liu and Ebrey, 1988) with a Nd-YAG laser with a polarization parallel with the bacteriorhodopsin alignment and intensity of 10 mJ as the excitation source. Measurements were made such that positive currents represent positive charge movement from the cytoplasmic side of the oriented membrane to the extracellular side and hence negative currents are a result of positive charges going in the opposite direction.

The buffer concentration was generally 5 mM with 50 μM $CaCl_2$ present unless otherwise noted. pH was adjusted by addition of small amounts of KOH or HCl. PM gels were equilibrated with the appropriate solutions by incubating them in a large volume of buffer at least overnight. The pH of the buffer solutions was remeasured at the time of the experiment because the pH's sometimes varied after incubation with the PM gels, especially when set beyond the buffering ranges of the solution.

Removal of divalent cations associated with the PM was accomplished by immersing the PM gel into a slurry of DOWEX 50W cation exchange resin (Bio-Rad Labs.-Chem. Div., Richmond, CA) and stirring overnight until the color changed to blue following Kobayashi et al. (1983). Subsequent incubation in the desired buffer and salt regenerated the purple color immediately for most cases. The exception arose with very low concentrations of $CaCl_2$. The equilibration rate with the salt was therefore determined by visual inspection of the gels. When deionized gels were placed in solutions with <5 μM $CaCl_2$ and at a pH of ~5.0, only the edges turned purple, while the center remained blue. The inhomogeneous color remained after 15 d of incubation. At pH 8, a homogeneous purple color returned immediately because of the pH. To see if the Ca^{2+} had been evenly distributed in the gel, we lowered the pH back to 5.0 after 5 d of incubation at pH 8.0; yet a blue center was again observed. The overall equilibration rate, however, is faster at high pH; an evenly colored gel can be obtained after 10 d incubation at pH 8.0. As a consequence of this behavior, regeneration of PM gels in low Ca^{2+} concentrations was conducted by shaking the gels in the Ca^{2+} solution with 5 mM GLY–GLY (pH 7.9) with daily changes for 15 d before measurements were taken.

Lipid-depleted PM gels were made as described by Liu et al. (1990) following the method of Szundi and Stoeckenius (1987). PM gels were incubated in 20 mM CHAPS (3-[(3cholamidopropyl)-dimethylammonio]-1-propanesulfonate) and 5 mM acetate buffer (pH 5.4) with stirring at room temperature and solution changes every 12 h for a total of 36 h. The detergent was removed by extensive rinsing of the gels with distilled water. Because the modification was conducted after the PM was immobilized in the polyacrylamide gel, lipid assays were not possible. As with our earlier description (Liu et al., 1990) the degree of delipidation was inferred by several physical properties of the lipid-depleted PM (absorbance maximum, M photointermediate decay lifetime, amplitude of M intermediate, lack of light/dark adaptation, and purple-to-blue transition) being the same as those described by others (Szundi and Stoeckenius, 1987; Jang and El-Sayed, 1988). Therefore, we assume that ~75% of lipids have been removed as assayed by Szundi and Stoeckenius (1987).

Arginine methyl ester modification of carboxyl groups was accomplished by placing PM gels in a constantly stirred solution of 100 mM arginine methyl ester and 0.5 M 1-ethyl-3-(3-dimethylaminopropyl) carbodiimide at room temperature for 4 h and pH 4.8 (Renthal et al., 1979) and renewing the solution after 2 h. Excess arginine methyl ester was removed with several changes of large volumes of distilled water.

The number of exponentials and lifetimes of the photocurrent and absorbance traces were determined by a program using nonlinear least squares subroutine CURFIT (Bevington, 1969) written for an LSI 11-23 minicomputer (Digital Equipment Corp., Maynard, MA). At each iteration of the fitting, the program is able to present both theoretical and experimental traces on the screen, so that the quality of the fitting could be judged not only by the standard deviation but also by the residual. When fitting traces containing a negative component of the buffer effect, a trace from an unbuffered PM gel containing 5 mM KCl was subtracted from the buffered traces such that what remained was a pure negative buffer signal that could be fit with two exponentials, a rise and decay. When fitting traces with a large positive component of the buffer effect, three exponentials were used, the first to fit the initial decay, the second for the rise due to the buffer, and the third for the longer overall decay.

RESULTS

Effect of the buffer charge transition on the photocurrent

31 buffers with pK's between 4.5 and 9.0 were tested for their influence on the photocurrent. These buffers are classified according to the type of charge transition they

undergo (Table 1). All affect the waveform of the B2 component if the salt concentration in the bathing solution is low enough (< 20 mM KCl or 5 mM $CaCl_2$). Although the waveform of the B2 component varies depending on type of buffer, its concentration, pH, and salt concentration, there are some general statements that can be made. The buffer effects can be divided into two types, N and P. The N (negative) buffer effect manifests itself as a microsecond photocurrent component such that the total current is more negative than the B2 waveform measured in a bufferless solution containing KCl at a concentration identical to that of the buffer

TABLE 1 Buffers classified according to charge transition characteristics

Buffer	Structure	pK
Type I (-3 → -2)		
Citrate	$^{-}O_2CCH_2C(OH)(CO_2^{-})CH_2CO_2^{-}$	5.4
Pyrophosphate	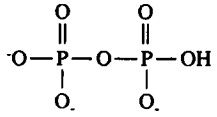	5.8
Type II (-2 → -1)		
Maleate	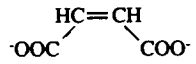	6.0
Phosphate	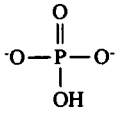	6.8
Phthalate	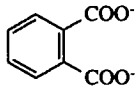	5.4
Succinate	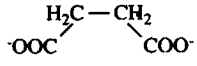	5.6
Type III (-1 → 0)		
Acetate	CH_3COO^{-}	4.8
Barbital	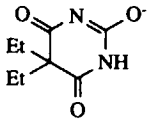	8.0
Bicarbonate	HCO_3^{-}	6.4
Cacodylate	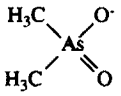	6.2
Type IV (-2 → -2 & +1)		
ADA	$H_2NCOCH_2N(CH_2COO^{-})_2$	6.6
PIPES	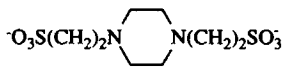	6.8
Type V (-1 → -1 & +1)		
ACES	$H_2NCOCH_2NH(CH_2)_2SO_3^{-}$	6.9
BES	$(HOCH_2)_2N(CH_2)_2SO_3^{-}$	7.2
BICINE	$(HO(CH_2)_2)_2NCH_2COO^{-}$	8.4
Type V (-1 → -1 and +1) (Cont.)		
GLY-GLY	$H_2NCH_2CONHCH_2COO^{-}$	8.4
Hepes	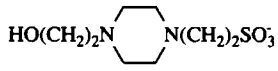	7.6
Hepps	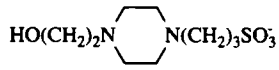	8.1
MES	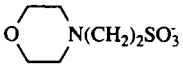	6.2
MOPS	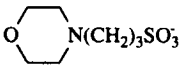	7.2
TAPS	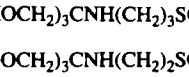	8.6
TES	$(HOCH_2)_3CNH(CH_2)_3SO_3^{-}$ $(HOCH_2)_3CNH(CH_2)_2SO_3^{-}$	7.5
TRICINE	$(HOCH_2)_3CNHCH_2COO^{-}$	8.2
TYPE VI (-1 & +1 → +2 & -1)		
Histidine	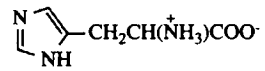	6.0
Type VII (0 → +1)		
Imidizole		7.1
Pyridine		5.1
Tris	$(HOCH_2)_3CNH_2$	8.3
Type VIII (+1 → +2)		
Bis-Tris Propane	$(HOCH_2)_3\overset{+}{C}\underset{H}{N}H(CH_2)_3NHC(CH_2OH)_3$	6.8
Ethylene Diamine	$H_2NCH_2CH_2\overset{+}{N}H_3$	7.5
Piperazine	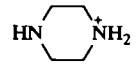	5.6
TEMED	$(CH_3)_2N(CH_2)_2\overset{+}{N}H(CH_3)_2$	6.0

at pH 6.0, usually ~5 mM. Conversely, the P (positive) buffer effect has a microsecond photocurrent component such that the total current is more positive than the B2 waveform measured in the same concentration of KCl, pH 6.0. The buffer component, therefore, is the difference between the photocurrents measured in buffer and in an equivalent concentration of KCl (pH 6.0). Although many factors affect the waveform of the buffer component, the most important is the type of charge transition during the protonation of the buffer molecules.

N effect

Of the buffers tested, only type VIII buffers produce an N effect. Upon protonation, the charge of a type VIII buffer changes from +1 to +2. Fig. 1, *a* and *b*, show the pH titration of B2 in the presence of 5 mM *bis-tris* propane pH buffer, pK 6.8. When the pH is low, B2 is basically the same as that in 5 mM KCl. With an increase in pH, however, B2 changes its waveform and even reverses signs. The new waveform can be described as the addition of a negative current component (N component) to B2; this change continues until the pH is much greater than the buffer's pK (Fig. 1 *b*).

P effect

Except for type VIII buffers, all of the other buffers tested show a P effect, the addition of a positive current component to the waveform of a B2 (Fig. 1, *c–k*). The exact waveform of the P component varies greatly. Some buffers such as ACES, phosphate, and glycylglycine (GLY–GLY) (Fig. 1, *c*, *f*, and *j*), show a clear notch in the microsecond range waveform; whereas others such as acetate, ADA, or bicarbonate (Fig. 1, *e*, *g*, and *h*) have a waveform that is only slightly more positive than that measured in 5 mM KCl. We discuss these buffers in groups by the type of charge transition.

(*a*) Type V buffers (Table 1) are zwitterionic pH buffers that carry only one pair of charges when protonated. All of the 11 buffers tested in this group showed a large P component. Fig. 1 *c* shows the pH titration of B2 in the presence of 5 mM ACES, and Fig. 1 *d* shows the same kind of titration in 5 mM MES. As can be seen, the effect of these zwitterionic buffers on the photocurrent is opposite to that of the N type buffers in that a new positive component is added to the B2. Its waveform is similar to the N component, but its polarity is positive. The amplitude of the P component increases with pH.

(*b*) Type IV buffers are zwitterionic and carry two negative and one positive charge in their protonated form. Only two of this type were tested. Both showed a small P effect, and their rise times were slow. Fig. 1 *e* shows the pH titration of the buffer ADA.

(*c*) Types II and III buffers behave similarly. Type II buffers have a −2 to −1 charge transition upon protonation, whereas type III buffers have a −1 to 0 charge transition upon protonation. Of the eight buffers tested in these two groups, phosphate, barbital, and cacodylate show large P components. Fig. 1 *f* shows a pH titration in 5 mM phosphate. Except for bicarbonate, the other types II and III buffers which have pK's <6.1 have small P components. Fig. 1 *g* shows the buffer effect of acetate. Although the pK of acetate is 4.8, the buffer effect does not start to appear until > pH 5.0 (see below). Fig. 1 *h* shows the buffer effect of 5 mM bicarbonate which behaves a little strangely. Although it has a pK of 6.4, the buffer component does not saturate at pH 7.4; it is still increasing at pH 8.2. The second protonatable group of bicarbonate (pK = 10.3) is presumably involved in which case there is now a type II buffer behavior (−2 to −1 charge transition).

(*d*) Type I buffers have a −3 to −2 charge transition upon protonation. Because of the large number of cations required as counter ions for these buffers upon pH adjustment, we reduced the buffer concentration to 1 mM so that the salt effect would not mask the buffer effect. Under these conditions, pyrophosphate showed a small P component. Citric acid had no effect on the B2, but an unusual photocurrent component with a lifetime about six times slower than the usual P component appeared (data not shown). Its origins are unknown.

(*e*) Only one type VI buffer was tested. Histidine is a zwitterionic buffer that carries two positive charges and one negative charge in its protonated form. It does not show a large buffer effect around its first pK of 6.0 (Fig. 1 *i*); however, it does show a large buffer effect at pH 7.7. Again, we presume the second protonatable group of histidine (pK = 9.17) is involved in a type V buffer effect (see above).

(*f*) Type VII buffers have a 0 to +1 charge transition during protonation. Of the three buffers tested in this group, imidazole and *tris* had somewhat resolvable P components whereas pyridine had only a small one.

(*g*) Type VIII buffers at higher pH's are now type VII buffers because the charge transition is 0 to +1. Therefore, measurements give a P type buffer effect after the N-type effect which had been seen at lower pH's. Fig. 1 *b* shows the pH titration of *bis-tris* propane in the pH 8.2–9.7 range. At pH's >8.2, the N component changes into a P component. At these pH's a second protonatable group (pK = 9.0) of *bis-tris* propane is being titrated.

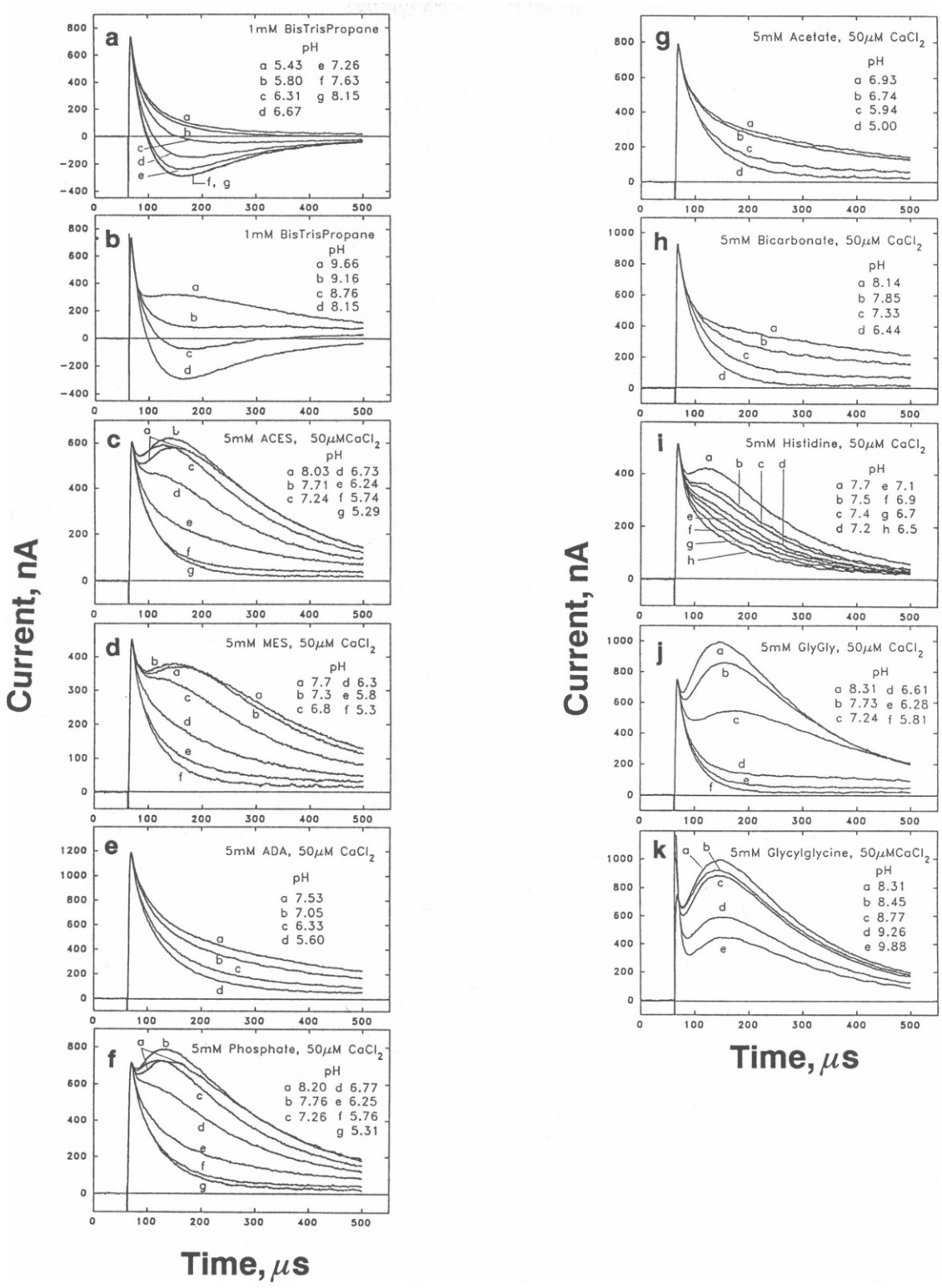

FIGURE 1 **Photocurrent of oriented PM gels as a function of pH in the presence of 19 of the 31 buffers tested.**

FACTORS THAT CONTROL THE AMPLITUDE OF THE BUFFER COMPONENT

pH and buffer pK

The buffer effect is pH dependent. As the pH increases, the buffer component usually starts to appear at pH 5.8 ± 0.3. At the concentration of PM used, 30 μM, there will be <15 μM protons released in the solution after each saturating flash (based on a quantum efficiency = 0.64 (Govindjee et al., 1990); and one proton per photocycle (Drachev et al., 1984)). It might be expected that this number of protons would make a significant disturbance to the pH of the solution even at pH 5 (where the bulk proton concentration is ~10 μM), but because pH is logarithmic, a concentration change of a factor of about two affects the pH very little. Furthermore, the local pH close to the surface of PM is much lower than the bulk pH. In the presence of 50 μM $CaCl_2$ with a bulk pH of 5.8, the pH in the solution next to the membrane where protonation of the buffer occurs is much lower than 5.0 (e.g., Jonas et al., 1990). Therefore, the release of <15 μM protons is probably not sufficient to cause the protonation of buffer molecules near the surface.

The amplitude of the buffer component usually starts to drop at pH 8.2 ± 0.3. Fig. 1 *k* shows this decrease in the pH titration of GLY–GLY in the pH 8.3–9.9 range. We suggest that this decrease is because of a lower number of protons available. Previously, we have found a drop in the number of protons released by a flash at this pH (Liu, 1990). That is, the decrease in amplitude here is attributed to the pK of the proton source, the purple membrane, not the pK of the buffer.

In addition, the pK of the buffer controls the buffer effect; however, it is difficult to sort this out. The measurements of the buffer components using buffers which have a pK in the 6.8–7.2 range, for example, could show a titration curve of their amplitudes even if they were due to a protein pK and independent of the protonation state of the buffers (i.e., their pK) because the buffer effect starts to increase at pH 5.8 and decrease at pH 8.2 for all buffers. This pH dependence could be due to the pH dependence of proton release from the PM at high pH and the lack of sufficient protons released to perturb the local proton concentration at low pH. After carefully examining the titration of MES (pK = 6.2) and GLY–GLY (pK = 8.4), however, we believe the buffer effect does depend on the buffer's pK. With higher pH's, the amplitude of the buffer component stops increasing when the buffer molecules are fully unprotonated. Comparing Fig. 1 *d* with Fig. 1, *j* and *k*, the pH titrations of MES and GLY–GLY, we can see that the buffer component in 5 mM MES becomes saturated at pH 7.3, one unit above its pK. The amplitude of the buffer component in 5 mM GLY–GLY increases up to pH 8.3, about the pH where the proton pumping ability starts to drop. The reason that the buffer component starts to appear at pH 6.3 even if the pK of GLY–GLY is at 8.4 is not clear. Perhaps, the protonation of the small amount of unprotonated GLY–GLY at pH 6.3 (40 μM with these conditions) induces this component.

The maximal amplitude of the P component also depends on the pK of the buffer. All the buffers that have a pK <6.0 induce a small P component, and all the buffers with a pK >6.0 induce a large P component with the exception of type IV buffers. The explanation is probably quite simple. As mentioned above, more protons are required to produce the same change in pH at lower pH's than at higher pH's. Thus, for a light-initiated release of a given amount of protons at a pH around the buffer pK, those buffers with lower pK's (e.g., <6) will have a smaller change in ratio of protonated and unprotonated buffer molecules than those with higher pK's and consequently less of a buffer-enhanced signal.

Salt concentration

The amplitude of the buffer component is sensitive to the cations surrounding the membranes. It starts to decrease as the cation concentration increases to a level comparable with that of the buffer. Divalent cations suppress the buffer component much more efficiently than monovalent cations. When starting with 5 mM buffer, 5 mM Ca^{2+} can significantly reduce the amplitude of the buffer component, but much more K^+ is needed for the same degree of reduction. Fig. 2 shows the buffer effect measured in 5 mM GLY–GLY with no added salt (GLY–GLY will contain ~1.4 mM of monovalent cations at pH 8.0), 5 mM KCl, or 5 mM $CaCl_2$ in the solution. A trace measured with 5 mM KCl alone is shown for comparison. Computer fitting of the traces indicates that the cations only reduce the amplitude of the buffer component without changing its decay kinetics.

Buffer concentration

The amplitude of the buffer component also depends on the concentration of buffer. Fig. 3, *a* and *b*, show the buffer concentration dependence of the P component of GLY–GLY and the N component of *bis-tris* propane, respectively. The N and P components have different concentration dependencies. The amplitude of the P

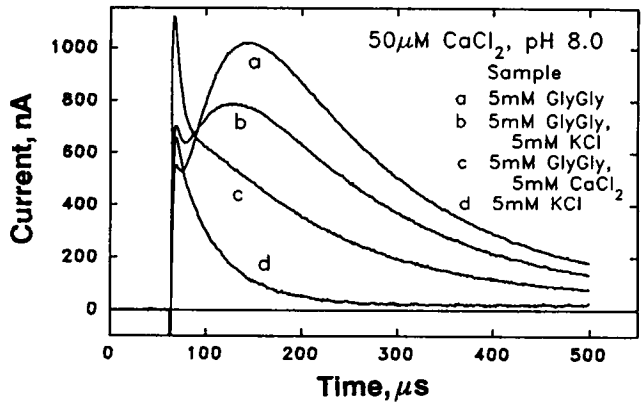

FIGURE 2 Effect of cations on the P-type buffer effect. B2 in only 5 mM GLY–GLY (*trace a*), in 5 mM GLY–GLY and 5 mM KCl (*trace b*), in 5 mM GLY–GLY and 5 mM $CaCl_2$ (*trace c*), and in 5 mM KCl only for comparison (*trace d*).

buffer component increases as the GLY–GLY concentration increases from 0.5 to 10 mM. The amplitude continues to increase a little above 10 mM, but at these concentrations it is difficult to separate the P component from the B2 component. One reason is that the higher concentration of buffer also causes the monovalent salt concentration to increase, which will cause B2 to become slower and larger (Liu et al., 1990). The second reason is that increasing the GLY–GLY concentration will increase the rate of the rise of the buffer component (see below). Consequently, we used 5 mM GLY–GLY for most of the studies presented here. At this concentration, the buffer component is clearly separated from B2 component, and the pH can still be well controlled.

For the N component, the amplitude decreases as the buffer concentration increases from 0.25 to 5 mM (Fig. 3 *a*). Tóth-Boconádi et al. (1986) report that the N effect reaches its maximum at 40–50 μM, which is ~100-fold lower than the concentration for a maximal P-type buffer effect (Fig. 3 *a*). An explanation of this difference is given in the Discussion. In this study, we used 1–2 mM *bis-tris* propane for most of our measurements of the N component. At lower concentrations, the pH is difficult to control and the buffer component is easily reduced by the contamination of small amounts of mono- or divalent cations; on the other hand, at higher concentrations the buffer component becomes smaller and hard to detect.

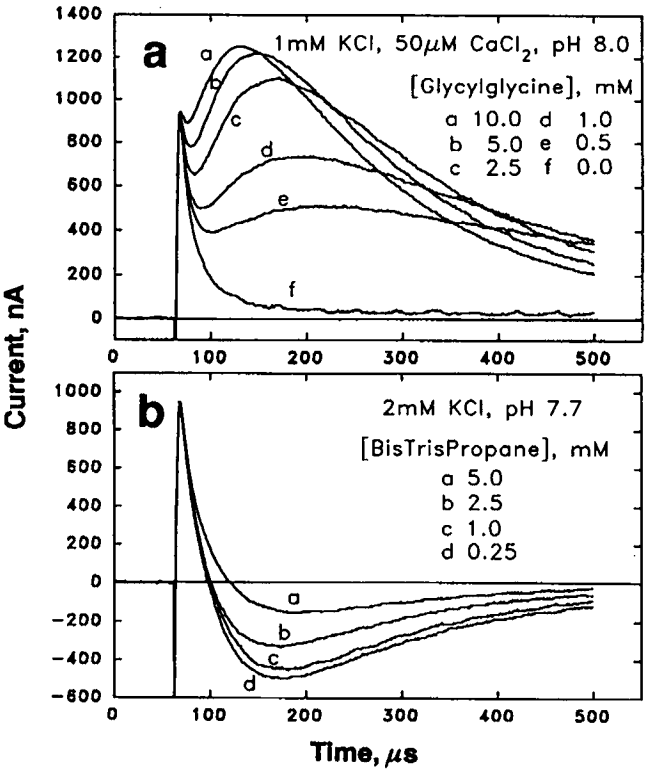

FIGURE 3 B2 as a function of buffer concentration as marked in the figure. (*a*) P-type buffer effect in different GLY–GLY concentrations. (*b*) N-type buffer effect in different concentrations of *bis-tris* propane.

Divalent cations in the binding site

Although the N component is not sensitive to micromolar concentrations of divalent cations (data not shown), the P component is. Fig. 4 *a* shows the P effect measured in 5 mM GLY–GLY at different concentrations of $CaCl_2$. The gels were first deionized to form blue membrane before they were incubated in the different Ca^{2+} solutions. The P component increases with higher Ca^{2+} concentration from <0.2 to 50 μM. Above 100 μM Ca^{2+}, the amplitude of the buffer component starts to drop because the higher concentrations of divalent cations inhibit the buffer effect (see above). At pH 8.0, 5 mM GLY–GLY contains 1.4 mM K^+(OH) used to adjust the pH. A comparison of the trace measured in <0.2 μM Ca^{2+} (see below) and in 0.2 μM Ca^{2+}, both of which contain the 1.4 mM K^+, shows that the 0.2 μM Ca^{2+} is more effective in increasing the P component than the 1.4 mM K^+, indicating that this divalent cation dependence is very specific.

There are almost certainly divalent cation binding sites on PM (see review of Jonas et al., 1990). According to Duñach et al. (1987), at pH 7.0, 1.8 μM concentration of Ca^{2+} would fill 90% of the high and middle affinity cation binding sites of PM under our experimental conditions, and 43 μM Ca^{2+} would fill 90% of the low affinity sites. From Fig. 4 *a*, we can see that the divalent cation dependence of the buffer component follows a very similar pattern to the divalent cation binding,

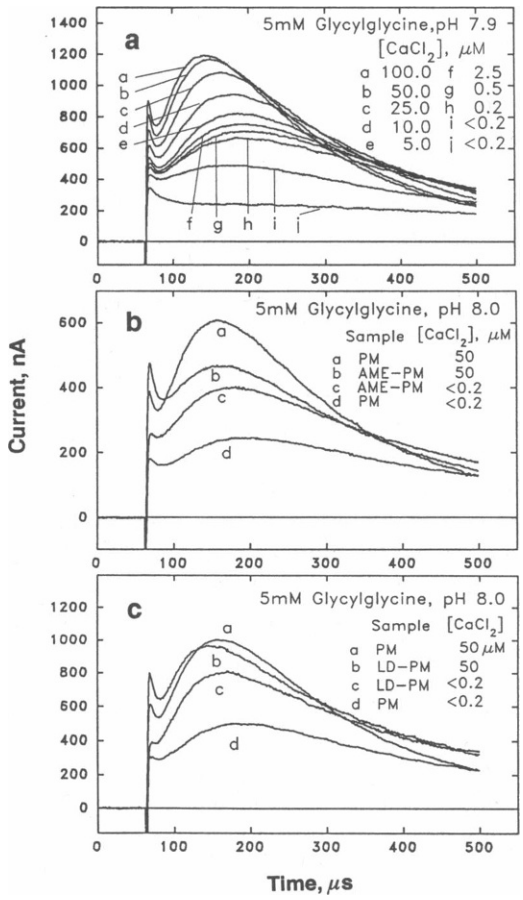

FIGURE 4 P type buffer effect. (*a*) Effect of different concentrations of Ca^{2+} on the amplitude. Traces i and j represent identical conditions of trace amounts of Ca^{2+} but i was incubated for 2 days, whereas j was incubated for 3 h; the longer time needed for binding of Ca^{2+} at low concentrations would explain for the increase in the P effect with time, but the 3 h trace reflects closer the trace in the absence of all divalent cations (see text). (*b*) Effect of chemical modifications of the negatively charged protein carboxylates with positively charged arginine methyl ester. Arginine methyl ester modification reduces the disparity between the minimal and maximal P effects due to Ca^{2+} concentration. (*c*) Effect of delipidation on the maximal and minimal Ca^{2+} signals. Reducing the number of negative charges from the lipids is similar to altering the amino acid residues where modification reduces the influence of Ca^{2+} on the amplitude of the buffer component. Where $<0.2\ \mu M\ Ca^{2+}$ is indicated, no Ca^{2+} was added to the solution but trace amounts were found to be present in the buffer solution at $<2\ \mu M$ as determined by inductively coupled argon plasma emission.

indicating that the divalent cations in the binding sites and in the Gouy-Chapman double layer might be important for the P effect. When the PM's surface potential was reduced by either covalently binding arginine methyl ester to carboxyl groups on the surface (Fig. 4 *b*) or by lipid depletion (Fig. 4 *c*), the membrane became less sensitive to the divalent cations in the solution.

The type of divalent cation appears not to be important. Comparison of the P components with $CaSO_4$ and $MgSO_4$ are basically the same except that the amplitude is slightly smaller in $MgSO_4$ (data not shown).

Aggregation states of PM

Sample conditions can affect the buffer waveform. Aggregation states of PM seem to have the biggest effect. PM which had been prepared and stored in a refrigerator three months before use had a lower molecular weight, increased light scattering, and smaller buffer components when compared to freshly made PM. Cleavage of the carboxyl terminal tail of bacteriorhodopsin has been seen in older preparations (Govindjee et al., 1982; Miercke et al., 1989), and the smaller protein has been found to aggregate (Arrio et al., 1986). Reduction of proton release signals in aggregated PM has also been reported previously with pH indicator experiments (Govindjee et al., 1982, 1984).

Other gel making conditions do not appear to affect the photocurrent signals. Specifically, pH (5.5–9.0), temperature (5–35°C), and acrylamide concentration (5–15%) were tested. At a pH of ~5, orientation of the PM was not possible; thus, there was no photocurrent signal. It is around this pH that the charge asymmetry of the PM changes (Fisher et al., 1978; Váró, 1981).

STUDY OF THE RISE AND DECAY PHASES OF THE BUFFER COMPONENT

Rate of rise

The rise time of the buffer component differs with type of buffer. It is not clear what determines this difference, but there seems to be a connection between the rate of rise and the pK of the buffer. For the 11 type V buffers tested, MES has the fastest rise time and TAPS the slowest when measured under similar conditions (data not shown). Table 1 shows that MES has the lowest pK and TAPS has the highest.

The rise time probably is related to the rate of release of protons from the membrane and the diffusion of these protons to the buffer molecules. A more detailed study of the rise times of two typical buffers, GLY–GLY and *bis-tris* propane, was done. The rate of rise of the P component of GLY–GLY shows a linear dependence on the concentration of the pH buffer (Fig. 5 *a*, *open circles*), suggesting that after a fixed time delay, part of the rise is a second order reaction proportional to the buffer concentration and that this part of the delay is diffusion controlled. Calculations using a typical value for diffusion-controlled second order rate constant of protonation from Gutman and Nachliel (1990), how-

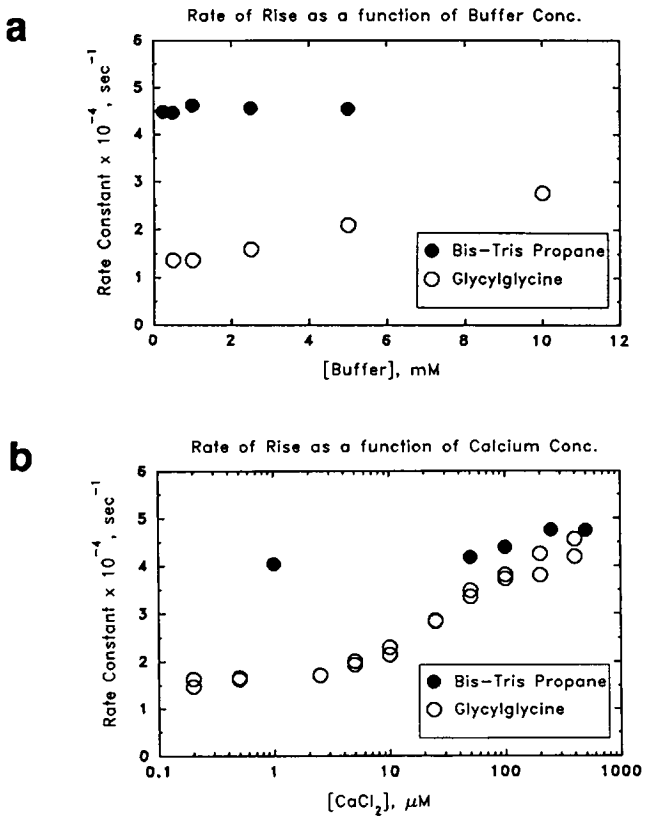

FIGURE 5 Rate constants of the rise of the buffer effect. (*a*) Rate of rise of the buffer component as a function of *bis-tris* propane, and GLY–GLY concentrations, and (*b*) Ca^{2+} concentration.

ever, indicate that the theoretical value for a diffusion-limited reaction of this type would be about three orders of magnitude faster than the rates of rise seen in these experiments. Thus, diffusion of protons cannot be the rate limiting step in this process due to the slower exponential release of protons from the protein. In contrast, the rate of rise of the N component of *bis-tris* propane is independent of the buffer concentration (Fig. 5 *a*, *solid circles*).

Fig. 5 *b* shows the effect on the rate of rise of N and P components of the concentration of $CaCl_2$. The rising rate of the N component is basically independent of the concentration of Ca^{2+} (Fig. 5 *b*). Without Ca^{2+}, the rate of rise of the P component is much slower than that of the N component. Higher Ca^{2+} concentrations increase the rate such that at 0.8 mM $CaCl_2$, the rising rate of the P component is about the same as that of the N component. An explanation based on different diffusion distances from the membrane is presented in the Discussion section.

Studies of the buffer component of PM which has had its surface potential reduced also suggest that proton diffusion controls part of the rising phase of the buffer component. Fig. 6 *a* shows that the rising phase of the N component of piperazine is significantly slowed down when some of the negatively charged carboxyl groups on the protein surface are converted into positively charged arginine groups. This charge change will greatly decrease the attraction of piperazine to the PM. This finding suggests that the farther the buffer is from the PM, the slower the rate of rise will be. The rise time of the P component of GLY–GLY of the modified PM also is shorter than that of the native PM under the identical conditions of no Ca^{2+} in the solution. With 50 μM Ca^{2+} at pH 8.0, the rising phase is about the same for arginine methyl ester modified PM and native PM (Fig. 4 *b*), perhaps because with the added Ca^{2+} the two samples have similar surface potentials.

The result of the reduction of the surface potential by lipid depletion is slightly different from the change seen in arginine methyl ester modified PM, perhaps suggesting that a more localized effect is occurring somewhere at the protein rather than an overall effect from the surface of the membrane and protein. The rise time of the GLY–GLY P component of lipid-depleted PM is shorter even in the presence of 50 μM Ca^{2+} than that of native PM under the same conditions (Fig. 4 *c*). The rise time of the N component did not change significantly upon lipid depletion (Fig. 6 *b*).

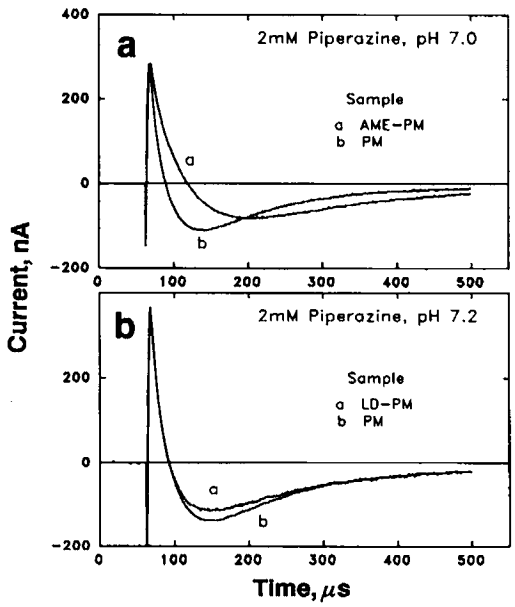

FIGURE 6 Effect of surface charge density modification on the N type buffer effect. (*a*) Modification of negative carboxylate groups with positively charged arginine methyl ester changes the rate of rise of the N component. (*b*) Removal of negatively charged lipids does not alter the N type signal in piperazine.

Decay phase

The decay rate of the buffer component differs somewhat from buffer to buffer. All except citrate have rates ranging from 0.2 to 0.7 $\times$ 10^4 s^{-1} at 20°C. For a specific buffer, the rate can also vary from one end of this range to the other depending on the measuring conditions (e.g., buffer concentration, divalent cations, etc. [see below]). This dependence on measuring conditions differs among buffers.

Fig. 7, *a* and *b*, (*solid symbols*) show that the decay rate of the N component of *bis-tris* propane is almost independent of both buffer concentration and the divalent cation concentration in the solution.

Fig. 7, *a* and *b*, (*open symbols*) show that the decay rate of the P component increases with the concentration of GLY–GLY or as the concentration of Ca^{2+} increases. In both cases, the rate reaches a limit of 0.6 $\times$ 10^4 s^{-1}, the same as the N effect.

The activation energy of the decay phase is similar to that of the L-M transition, indicating the two processes

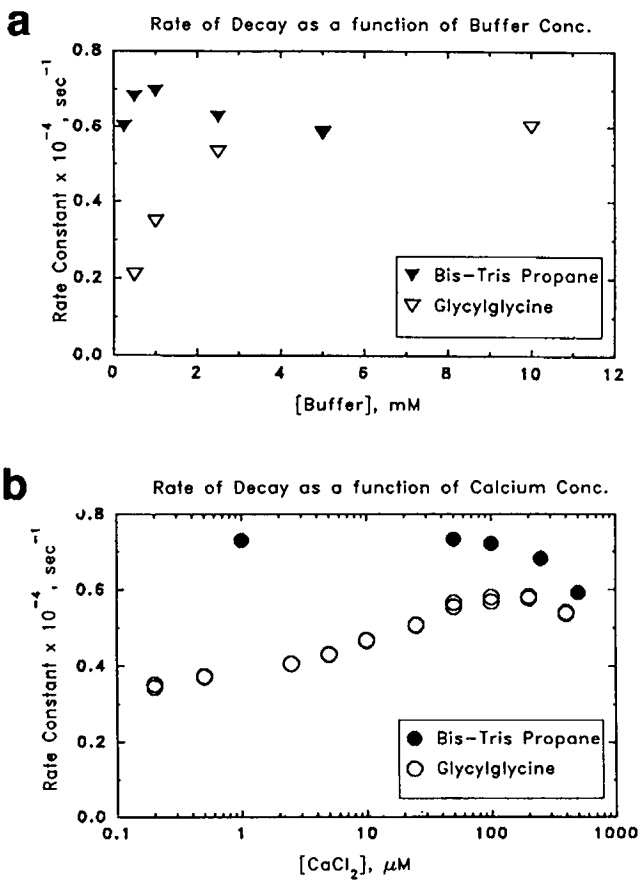

FIGURE 7 Rate of decay of the buffer component as a function of (*a*) buffer concentration and (*b*) as a function of the Ca^{2+} concentration.

are closely correlated (data not shown). Identical activation energies for B2 were also seen in its normal and modified by low salt conditions forms (Liu et al., 1990). We do not understand why the buffer decay phase is slower than the L-M transition, and why the decay rates of some buffers that produce a P effect are much slower than others.

DISCUSSION

The data presented above indicate that when the salt and buffer concentrations are relatively low, the microsecond photocurrent component, B2, becomes very sensitive to the presence of a buffer. It appears that a buffer adds a photocurrent component to the intrinsic photocurrent component. In studying these buffer components, we have formulated a theory that can explain most of the phenomena presented.

Although the N and P components have different polarities and many small differences, the following points indicate they are closely related. Both the N and P components are significantly reduced when a comparable concentration of divalent cations is present. Both the N and P components are reduced when the gels are made of aggregated PM. Both N and P components follow similar amplitude dependencies on the pH. At moderate divalent cation concentrations, both the rise (and decay) rates of the N and P components are the same (Figs. 5 *b* and 7 *b*). Therefore, we think P and N components have a similar origin. From the data for all the buffers (Table 1), we find that the N effect is induced by positively charged buffers whereas the P effect is induced by negatively or uncharged buffers.

Three types of evidence suggest that protonation of buffer molecules is the basic event leading to the buffer effect. First, only pH buffers have this effect on the photocurrent; tetraethylammonium, a relatively large organic cation of similar size to the buffers tested, does not produce a buffer component. In fact the waveform of the photocurrent in the presence of tetraethylammonium chloride is the same as that in KCl (data not shown). This observation indicates that the N and P effects are specific for pH buffer molecules. Secondly, the amplitude of the buffer component depends on its pK and is maximal when the buffer is entirely in its unprotonated form. As noted above, buffers which have a pK <6.0 also produce smaller P components. We have suggested this may be because the amount of protons produced at these lower pH's does little to perturb the proton concentration and hence does not significantly protonate a large fraction of the unprotonated buffer molecules. Finally, whether a buffer will produce an N or P buffer effect depends on the type of charge transition

upon protonation. Over the pH range in which *bis-tris* propane has a type VIII transition (+1 to +2), an N buffer components is observed (Fig. 1 *a*), but over the pH range in which *bis-tris* propane acts as a type VII buffer (0 to +1 charge transition), a P component is observed (Fig. 1 *b*). Based on these results, we think it is quite likely that the buffer component is induced by the protonation of the buffer molecules, presumably by light-induced proton release from the PM.

This buffer protonation process probably happens in solution close to the surface of bacteriorhodopsin based on the following evidence. Gels made of aggregated PM produce smaller buffer effects, suggesting the protonation happens in solution close to the surface of membrane. Aggregation of PM would prevent buffers from moving freely near the membrane surface. Furthermore, there is no evidence that buffers can get inside bacteriorhodopsin or bind to the surface of PM. Types I, II, III, IV, and V buffers are negatively charged before they are protonated and will be repelled from the negatively charged PM. In addition, when the surface potential is high, the rise time of the N component (due to positively charged buffers) is faster than the P component (due to negatively charged or zwitterionic buffers). When the surface potential is reduced by adding Ca^{2+} in the solution, the rise times of the N and P components become equal (Fig. 5 *b*). We have suggested in Results that the rate of rise is partially determined by the rate of proton release and the rate that the protons protonate the buffer molecules by diffusing to them. If so, the rate difference would be because *bis-tris* propane (type VIII) is positively charged and GLY–GLY (type V) is negatively charged. It will take longer for the protons to reach the GLY–GLY than the *bis-tris* propane molecules.

A model can explain most of our photocurrent observations in terms of the protonation of buffer molecules in the solution near the surface of PM. Previously, we have suggested that when measuring the photocurrent in low salt a counter current is induced by the cations in the solution to compensate for the negative charge created on the membrane due to proton release (Liu et al., 1990). This counter current model should also apply with the buffer solutions. The metal cations that accompany the buffer and the positively charged type VIII buffers will form a counter current and cause B2 to appear faster, as with the regular salt effect. However, the protonation of buffer molecules will cause an additional counter current component, the buffer component. Below are two possible sources for this additional current component. Both probably contribute.

Upon protonation the less negatively charged buffer molecules move toward the surface of the membrane. When type VIII buffers move, they will induce a negative current because they are positively charged. Conversely, the negatively charged types I, II, and IV buffers will move toward the negatively charged membrane because they become less negative upon protonation; this movement of a negative charge in this direction will result in a positive current. The results with buffer types III and V are a little harder to explain as being due to a protonation followed by movement because, whereas negative before protonation, the resulting charge is neutral. The primary problem with this model for the buffer behavior is that buffer types VI and VII, which have a net positive charge upon protonation, still produce a P component.

To account for problems in the above explanation, we propose that there is at least one other source for the buffer-induced current. The change in dipole moment of the buffer upon protonation will result in current changes which could add to or subtract from the proton current. The dipole moment of a buffer molecule should be aligned near the surface of PM. Protonation of the buffer will cause an alteration of its dipole moment and thus a rotation of the charged molecule, causing a new current component. Two observations suggest this possibility. First, of the 27 buffers that induce a P component, that of GLY–GLY is the largest. Before protonation, GLY–GLY is expected to have a dipole very similar to the other type V buffers. After protonation, GLY–GLY will have a much larger dipole moment because the charge is separated by two amino acids (see Table 1). Therefore, the dipole change of the buffer is also expected to be very large. Second, the structure and many properties of type IV buffers are very similar to type V buffers; however, type IV comprises a unique buffer group that produces small P components that are very different from the type V buffers. A comparison of the structures of the type IV and V buffers suggests that the former will have a smaller dipole change than the latter. However, because we do not know precisely how the dipoles are aligned and how they will change, the contribution of such dipole changes is difficult to quantitate.

Several observations that we made can be readily explained by the combination of the high negative charge carried by the PM over the measured pH range and the charges carried by the buffers. For example, the reduced amplitude of the N (Fig. 3 *b*) and P (figure not shown) components with increasing buffer concentration occurs because both types of buffers will contain significant concentrations of cations, either because the buffers are cations or because cations are added to adjust the pH of the solution. These will act as counterions, in the same manner as increased salt concentration (Liu et al., 1990) and thus reduce the counter current due to the buffer molecules. Another example is the different concentrations at which the N type and P type

buffers have their maximal effect. The N type buffers have their maximal effect at 50 μM (Tóth-Boconádi et al., 1986), whereas the P type buffers have theirs at 10 mM (Fig. 3 *a*). The type VIII buffers which give rise to the N effect are positively charged and hence will be close to the membrane surface. Indeed, under our conditions their surface concentration will be many orders of magnitude higher than their bulk concentration of 50 μM and thus about equal to the surface concentration of the negatively charged and uncharged buffers that give rise to the P effect whose bulk concentration is 10 mM. A third set of experiments that can be understood in terms of simple electrostatics is the effect of added divalent cations on the amplitudes of the N and P buffer components. The added divalents will reduce the surface potential of the PM both by reducing the surface charge density by binding and by acting as free Gouy-Chapman cations in the double layer (Jonas et al., 1990). The reduced surface potential will allow the negatively charged buffer molecules to move closer to the surface (see Fig. 4 *a*), explaining their large effects on these buffer components which give rise to the P effect. As noted in Results (Fig. 4, *b* and *c*), reducing the surface potential by chemical means also reduces the effect of the divalent cations, as would be expected if the cationic effect is through modulation of the surface potential. In contrast to the P current, the N current was not sensitive to divalent cations, presumably because the positively charged type VIII buffers will always be near the surface of the membrane (or have high surface concentrations) at all the bulk concentrations examined. Finally, in studying the effect of buffer concentration on the rate of rise and decay of the buffer effect, we suggested that proton diffusion to the buffer molecules was a contributing component. That the rise and decay rates were independent of buffer concentration for the positively charged type VIII buffers would again be due to the high local concentration of these buffers next to the membrane, so that the diffusion times were no longer a factor. In contrast, the rise time of the P component speeds up with increasing Ca^{2+} concentration until it is equal to the rise time of the N component (Fig. 5 *b*).

Although much can be explained by the model presented above, a full explanation of all the effects of buffers on the photocurrent is still lacking. The rising phase of the P component appears to depend partially on the buffer concentration and on the distance of buffer molecule from the membrane; yet, as mentioned above, calculations indicate that this alone cannot be the rate limiting step as the experimental rate is at least three orders of magnitude too slow to be limited by the diffusion distance and protonation rate of buffer molecules. It is not quite clear what controls the decay rate of the buffer component. Nor is it clear why the rising rate of the P component is different for different buffers when the conditions used are the same. Gutman and Nachliel (1990) state that the protonation rate is basically independent of pK whereas the deprotonation rate has a linear relationship with the pK, but our data clearly show the buffer effect is a protonation process. Finally, it is not clear why the rate of rise of N component for lipid-depleted PM, which has a reduced surface potential, does not decrease other than the possibility that the observed effect is more sensitive to the protein surface rather than the overall negative lipid surface.

Although we do not understand all the phenomena we observe in the photocurrent measurements, it is evident that these currents are very sensitive to molecules and ions in the solution surrounding the membrane. Here we have provided a systematic description of the effects of pH buffers and given a possible mechanism for how the photocurrent is affected by the buffers.

The authors would like to thank Barbara Jonas for the preparation of the purple membrane.

M. Kono was partially supported by National Institutes of Health Molecular Biophysics Training grant 5T32 GM08276-02. This work was supported by the Department of Energy grant F002-88ER13948 and National Science Foundation grant DMB 881524 to T. G. Ebrey.

Received for publication 12 October 1990 and in final form 18 March 1991.

REFERENCES

Arrio, B., G. Johannin, P. Volfin, M. Lefort-Tran, L. Packer, A. E. Robinson, and E. Hrabeta. 1986. Aggregation and proton release of purple and white membranes following cleavage of the carboxyl-terminal tail of bacteriorhodopsin. *Arch. Biochem. Biophys.* 246:185–191.

Becher, B., and J. Y. Cassim. 1975. Improved isolation procedures for the purple membrane of *Halobacterium halobium*. *Prep. Biochem.* 5:161–178.

Bevington, P. R. 1969. Data Reduction and Error Analysis for the Physical Sciences. McGraw-Hill Inc., New York. 237–239, 302–303.

Dér, A., P. Hargittai, and J. Simon. 1985. Time-resolved photoelectric and absorption signals from oriented purple membranes immobilized in gel. *J. Biochem. Biophys. Methods.* 10:259–300.

Dér, A., R. Tóth-Boconádi, and L. Keszthelyi. 1988. Counterions and the bacteriorhodopsin proton pump. *FEBS (Fed. Eur. Biochem. Soc.) Lett.* 229:313–316.

Drachev, L. A., A. D. Kaulen, and V. P. Skulachev. 1984. Correlation of photochemical cycle, H^+ release and uptake, and electric events in bacteriorhodopsin. *FEBS (Fed. Eur. Biochem. Soc.) Lett.* 178:331–335.

Duñach, M., M. Seigneuret, J.-L. Rigaud, and E. Padros. 1987. Characterization of the cation binding sites of the purple mem-

brane. Electron spin resonance and flash photolysis studies. *Biochemistry.* 26:1179–1186.

Fisher, K. A., K. Yanagimoto, and W. Stoeckenius. 1978. Oriented adsorption of purple membrane to cationic surfaces. *J. Cell Biol.* 77:611–621.

Govindjee, R., K. Ohno, and T. G. Ebrey. 1982. Effect of the removal of the COOH-terminal region of bacteriorhodopsin on its light-induced H^+ changes. *Biophys. J.* 38:85–87.

Govindjee, R., K. Ohno, C.-H. Chang, and T. G. Ebrey. 1984. The C-terminal tail of bacteriorhodopsin—its conformation and role in proton pumping. *In* Information and Energy Transduction in Biological Membranes. C. L. Bolis, E. J. M. Helmreich, and H. Passow, editors. Alan R. Liss, Inc., New York. 13–25.

Govindjee, R., S. P. Balashov, and T. G. Ebrey. 1990. Quantum efficiency of the photochemical cycle of bacteriorhodopsin. *Biophys. J.* 58:597–608.

Gutman, M., and E. Nachliel. 1990. The dynamic aspects of proton transfer processes. *Biochim. Biophys. Acta.* 1015:391–414.

Jang, D.-J., and M. A. El-Sayed. 1988. Deprotonation of lipid-depleted bacteriorhodopsin. *Proc. Natl. Acad. Sci. USA.* 85:5918–5922.

Jonas, R., Y. Koutalos, and T. G. Ebrey. 1990. Purple membrane: Surface charge density and the multiple effect of pH and cations. *Photochem. Photobiol.* 52:1163–1177.

Keszthelyi, L., and P. Ormos. 1989. Protein electric response signals from dielectrically polarized systems. *J. Membr. Biol.* 109:193–200.

Kobayashi, T., H. Ohtani, J. Iwai, A. Ikegami, and H. Uchiki. 1983. Effect of pH on the photoreaction cycles of bacteriorhodopsin. *FEBS (Fed. Eur. Biochem. Soc.) Lett.* 162:197–200.

Liu, S. Y. 1990. Light-induced currents from oriented purple membrane. I. Correlation of the microsecond component (B2) with the L-M photocycle transition. *Biophys. J.* 57:943–950.

Liu, S. Y., and T. G. Ebrey. 1988. Photocurrent measurements of the purple membrane oriented in a polyacrylamide gel. *Biophys. J.* 54:321–329.

Liu, S. Y., R. Govindjee, and T. G. Ebrey. 1990. Light-induced currents from oriented purple membrane. II. Proton and cation contributions to the photocurrent. *Biophys. J.* 57:951–963.

Marinetti, T. 1987. Counterion collapse and the effect of diamines on bacteriorhodopsin. *FEBS (Fed. Eur. Biochem. Soc.) Lett.* 216:155–158.

Marinetti, T., and D. Mauzerall. 1983. Absolute quantum yields and proof of proton and nonproton transient release and uptake in photoexcited bacteriorhodopsin. *Proc. Natl. Acad. Sci. USA.* 80:178–180.

Miercke, L. J. W., P. E. Ross, R. M. Stroud, and E. A. Dratz. 1989. Purification of bacteriorhodopsin and characterization of mature and partially processed forms. *J. Biol. Chem.* 264:7531–7535.

Renthal, R., G. J. Harris, and R. Parrish. 1979. Reaction of the purple membrane with a carbodiimide. *Biochim. Biophys. Acta.* 547:258–269.

Szundi, I., and W. Stoeckenius. 1987. Effect of lipid surface charges on the purple-to-blue transition of bacteriorhodopsin. *Proc. Natl. Acad. Sci. USA.* 84:3681–3684.

Tóth-Boconádi, R., S. G. Hristova, and L. Keszthelyi. 1986. Diamines reverse the direction on the bacteriorhodopsin proton pump. *FEBS (Fed. Eur. Biochem. Soc.) Lett.* 195:164–168.

Trissl, H.-W. 1990. Photoelectric measurements of purple membranes. *Photochem. Photobiol.* 51:793–818.

Váró, Gy. 1981. Dried oriented purple membrane samples. *Acta Biol. Acad. Sci. Hung.* 32:301–310.